07.1

Features of the current-voltage characteristic of the Ti−Si@O@Al junction Ti−Si@O@Al

© A.S. Rudy, A.B. Churilov, A.A. Mironrenko, V.V. Naumov, S.V. Kurbatov, E.A. Kozlov

Demidov State University, Yaroslavl, Russia
E-mail: rudy@uniyar.ac.ru

Received June 8, 2022
Revised June 8, 2022
Accepted July 13, 2022

The results on measuring the I–V characteristics of the metal−semiconductor transition within the Ti (200 nm)—Si@O@Al (180 nm)—Ti (203 nm) test structure are presented. The basis of the Si@O@Al nanocomposite is a solid solution of Al in amorphous silicon *a*-Si(Al). The I–V of the test structure has a form characteristic of a reverse-biased ohmic contact between a metal and a *p*-type semiconductor, which implies that *a*-Si(Al) is a substitutional solid solution. It is shown that the I–V fits well the framework of the metal-semiconductor transition model and the varistor effect of the nanocomposite. Within the framework of the percolation model, it is shown that the I–V give values of the Si@O@Al resistivity, which are overestimated with respect to the resistance of the *a*-Si(Al) solid solution.

Keywords: nanocomposite, amorphous silicon, solid solution, Schottky barrier, nonlinear conductor, dangling bonds.

DOI: 10.21883/TPL.2022.09.55072.19276

Microelectronics and photovoltaics have traditionally been regarded as the primary application niches of silicon. Owing to its capacity for reversible intercalation of large amounts of lithium, silicon is now being used more and more widely in the design of lithium-ion batteries. A single silicon atom is theoretically capable of retaining up to 4.4 lithium atoms ($Li_{22}Si_5$). This corresponds to a capacity of 4200 mA · h/g. However, such parameters are infeasible in practice, since the resulting internal stresses literally pulverize crystalline silicon. Therefore, a special nanocomposite Si@O@Al material (Si ∼ 70%, O — 15−20%, Al — 10−15%) was designed for solid-state lithium-ion batteries [1,2]. The capacity of this nanocomposite is somewhat lower, but it is more stable, features high hole and ion conductivity values, and strong adhesion to metals and the LiPON solid electrolyte.

Si@O@Al features a number of properties that are novel for a nanocomposite and manifest themselves when it is used as a component of thin-film solid-state lithium-ion batteries. For example, the emergence of a hike on the charging curve was reported in [3]. This effect is attributable to a change in the conductivity type of *a*-Si(Al), which is the conductive framework of Si@O@Al. It was hypothesized in [3] that undoped *a*-Si(Al), where Al is the dissolved component of an interstitial solid solution, is a *p*-type semiconductor. In the process of lithiation, *a*-Si(Al) turns into *a*-Si(Li), the semiconductor becomes compensated, and eventually the conductivity type changes. A forward-biased Ti—*a*-Si(Al) Ohmic contact thus turns into a reverse-biased Ti—*a*-Si(Li) rectifying contact. This is the reason why the current through the Ti—*a*-Si(Li) junction is produced by minority carriers (holes) and electrons that need to overcome the Schottky barrier from the metal side. A galvanostat raises the potential in order to maintain the galvanostatic mode, and a hike emerges on the charging curve as a result.

Test Ti—Si@O@Al—Ti structures with a lateral size of 1 × 1 cm were fabricated in order to determine whether the *a*-Si(Al) solid solution does indeed feature hole conductivity. The cleaved face of the test structure (with the thickness of its layers indicated) is shown in Fig. 1. Since the Si@O@Al nanocomposite in these structures does not contain Li, it should, in accordance with the model presented in [3], be a *p*-type semiconductor. The Fermi level in a semiconductor of this kind is located close to the hole mobility gap (Fig. 2), and an enriched hole layer forms in the junction region. Under forward bias (minus at Ti), the primary conductivity mechanism is then the recombination of holes at the interface, and the I–V characteristic is linear in nature. The junction resistance is low, and the voltage drops

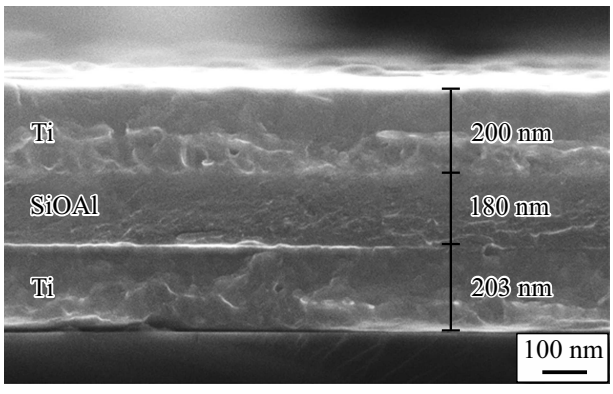

Figure 1. The cleaved face of the test structure Ti—Si@O@Al—Ti.

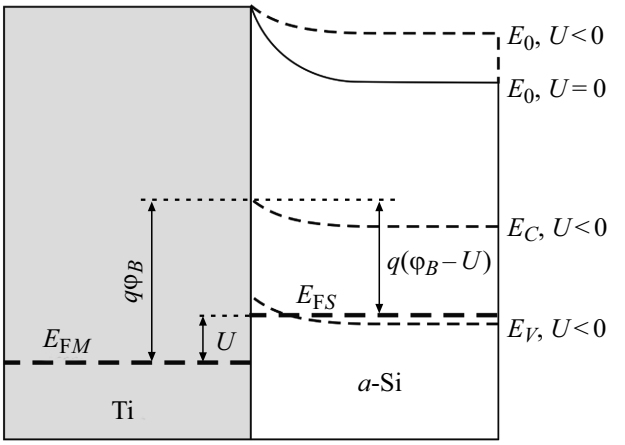

Figure 2. Band diagram of a reverse-biased Ti−a-Si(Al) contact (plus at Ti). E_{FM} is the Fermi level of titanium, E_{FS} is the Fermi level of amorphous silicon, and E_C, E_V are the mobility threshold energies (relative to vacuum).

entirely within the bulk of Si@O@Al. When the polarity is reversed, majority carriers shift away from the interface, while minority carriers (electrons) move into the metal, overcoming potential barrier $q\varphi_B = A_M - \chi$, where A_M is the work function of the metal and χ is the electron affinity of the semiconductor (Fig. 2). Since the net current in the test Ti—Si@O@Al—Ti structure is limited at all times by the reverse-biased junction (plus at Ti), its I–V characteristic always has the form of an I–V curve of a reverse-biased junction.

Figure 3, a shows the I–V characteristic of the test Ti—Si@O@Al—Ti structure (solid curve) measured by cyclic voltammetry at a scan rate of 5 mV/s. Let us demonstrate that the experimental curve is characterized well by the Richardson formula [4] for a reverse-biased metal–semiconductor junction

$$I = I_s\left(e^{\frac{q(U-U_V)}{k_BT}} - 1\right), \tag{1}$$

where $I_s = AT^2e^{-\frac{q\varphi_B}{k_BT}}$ is the saturation current density, A is the thermoelectric constant (Richardson constant), $q\varphi_B$ is the Schottky barrier height, U is the bias voltage, and U_V is the voltage drop across the Si@O@Al layer.

It can be seen from Fig. 3, a that the resistance of the bulk of the nanocomposite is nonlinear in nature and may be characterized by expression

$$U_V = R^*I^\alpha + R_0I, \tag{2}$$

where R^* is a coefficient expressed in units of $\Omega \cdot \mathrm{A}^{1-\alpha}$ [5], R_0 is the residual resistance, and α is a quantity reciprocal to coefficient $\beta = (U/I)(dI/dU)$ of the I–V characteristic nonlinearity factor. Neglecting the R_0I term due to its smallness, we transform expression (1) into the form

$$I = I_s\left(e^{\frac{q(U-R^*I^\alpha)}{k_BT}} - 1\right). \tag{3}$$

In order to plot an I–V characteristic of the junction in the traditional form of $I(U)$, we turn to the inverse dependence, which takes the form

$$U = \frac{k_BT}{q}\ln\left(1 + \frac{I}{I_s}\right) + R^*I^\alpha. \tag{4}$$

Inversed dependence (4) is also shown in Fig. 3, a (open circles). According to the presented curves, dependence (4). Properly characterizes the experimental (solid) curve within the indicated voltage range. This implies that unlithiated Si@O@Al features p-type conductivity and is a nonlinear material.

Fitting parameter I_s allows one to determine Schottky barrier height $\varphi_B = \ln(AT^2/I_s)(k_BT/q)$, which assumes the value of 1.0 V in the present case. This height was estimated in [3] at 2.0 V based on the results reported in [6,7]. The reasons behind this discrepancy are quite obvious. The first one is the uncertainty of the work function of titanium, which may vary by up to 0.4 eV depending on the surface condition. The second reason is the deviation of the electron affinity of the a-Si(Al) solid solution from the electron affinity of the model a-Si system examined in [6,7].

The nonlinear current dependence of the Si@O@Al resistance

$$R = R^*I^{\alpha-1} + R_0, \tag{5}$$

which is termed the varistor effect [5,8], is due to the composite nature of Si@O@Al. The key difference between Si@O@AL and traditional varistor materials consists in the fact that it lacks filler in the shape of uniform particles or their agglomerates. Column-shaped a-Si(Al) blocks, which are separated partially from each other by vertical pores, may be regarded as filler, and the separating voids, pores, and molecular SiO_2 clusters may be seen as dispersing agents. In addition to a-Si(Al), columns contain molecular SiO_2 clusters and are heterogeneous as well (Fig. 3, b). This is evidenced by the data from [9]. According to the results reported there, the morphology of a Si@O@Al film remains unchanged after etching in a fluoric acid solution, but its ion conductivity increases significantly.

Expression (5) provides an opportunity to estimate the minimum resistance in the 0−0.08 A range. It yields, up to an unknown constant R_0, $R = 6.26\,\Omega$ (or $\sigma = 2.86 \cdot 10^{-4}\,\mathrm{S \cdot m^{-1}}$) for $R^* = 1.56\,\Omega \cdot \mathrm{A}^{1-\alpha}$ and $\alpha = 0.45$. Since this result agrees with the experimental data from [10] and several other studies, the added aluminum ostensibly produces only a negligible contribution to the hole conductivity. In actual fact, the I–V characteristic and dependence (5) derived from it overestimate the resistance value. This is illustrated by the two-dimensional percolation model in Fig. 3, b. Gray cells in this model represent the regions composed primarily of a-Si(Al), while white cells mostly contain SiO_2 and voids. Thick lines are the trajectories of current flow; the resistivity of Si@O@Al along them may exceed the resistivity of a-Si(Al) by several orders of magnitude.

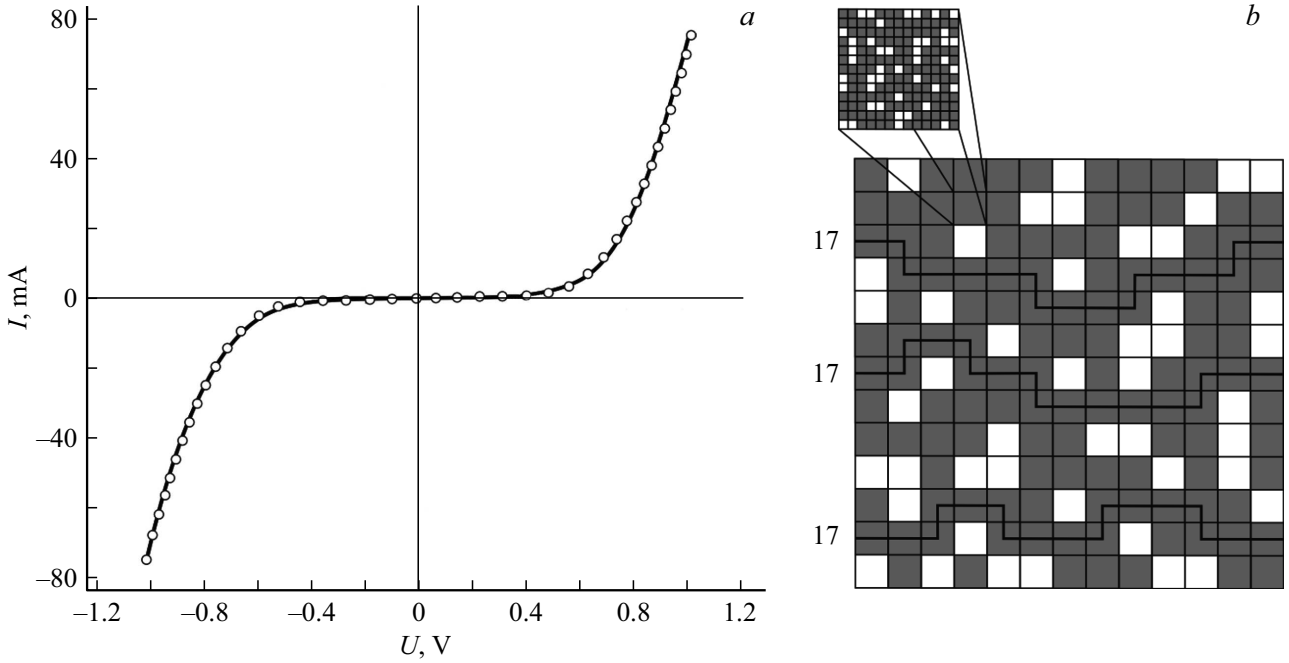

Figure 3. *a* — I–V characteristic of the test Ti—Si@O@Al—Ti structure with an area of 1 cm^2 measured at a scan rate of 5 mV/s (solid curve) and inversed dependence (4) (open circles) for parameters $I_s = 10^{-10}$A · cm^{-2}, $R^* = 1.56\,\Omega \cdot A^{1-\alpha}$, $\alpha = 0.45$. *b* — Percolation model of the Si@O@Al nanocomposite. Gray cells are regions dominated by *a*-Si(Al), and white cells are dispersing regions formed by SiO_2 and voids. Solid lines represent flow trajectories; the number of cells through which a given trajectory goes is indicated on the left.

Since Al atoms, owing to the specifics of their electron configuration, may saturate dangling bonds only by forming a substitutional *a*-Si(Al) solid solution [3], this should also lead to an enhancement of the crystallinity of Si@O@Al. However, according to the X-ray diffraction analysis data, the degree of ordering of amorphous silicon is defined primarily by the deposition rate, and any crystallinity variations induced by the addition of Al are rather hard to discern against this background. It is theoretically possible for dangling bonds to be saturated by bridging oxygen Si–O–Si. Indeed, the length of a Si–O–Si siloxane chain is 3.28 Å, while the length of a Si–Si bond is 3.24 Å. This makes the formation of Si–O–Si at the defect site possible. That said, the bond angle is 142.5° [11]; i.e., the structural defect itself may be retained after the formation of a siloxane bond. At the oxygen concentration given in [3], the formation of molecular SiO_2 clusters appears to be more probable.

The presumed formation of molecular clusters agrees well with the fact that a varistor effect was observed. This effect finds its explanation within the cluster model of Si@O@Al, where nanoparticles of the *a*-Si(Al) solid solution act as filler, while voids and silicon dioxide clusters serve as dispersing agents. Thus, the experimentally determined resistance of Si@O@Al is actually the resistance of a highly branched system of percolation clusters. This precludes one from calculating the resistivity of the *a*-Si(Al) solid solution and comparing it to the resistivity of *a*-Si and *a*-Si:H.

Acknowledgments

Equipment provided by the „Diagnostics of Micro- and Nanostructures“ common use center was used in the study.

Funding

The study was supported financially by the Ministry of Science and Higher Education of the Russian Federation under state assignment No. 0856-2020-0006 for the Demidov Yaroslavl State University.

Conflict of interest

The authors declare that they have no conflict of interest.

References

[1] A.A. Mironenko, I.S. Fedorov, A.S. Rudy, V.N. Andreev, D.Yu. Gryzlov, T.L. Kulova, A.M. Skundin, Monatsh. Chem. — Chem. Monthly, **150** (10), 1753 (2019). DOI: 10.1007/s00706-019-02497-1

[2] T.L. Kulova, A.A. Mironenko, A.S. Rudy, A.M. Skundin, *All solid state thin-film lithium-ion batteries. Materials, technology, and diagnostics* (CRC Press, Boca Raton, 2021). DOI: 10.1201/9780429023736

[3] A.S. Rudyi, A.A. Mironenko, V.V. Naumov, A.B. Churilov, Pis'ma Zh. Tekh. Fiz., **48** (12), 32 (2022) (in Russian). DOI: 10.21883/PJTF.2022.12.52676.19188

[4] M. Shur, *Physics of semiconductor devices* (Prentice-Hall, N.J., 1990), p. 197.

[5] M.K. Kerimov, M.A. Kurbanov, I.S. Sultanahmedova, I.A. Faradzhzade, F.N. Tatardar, H.S. Aliyev, F.F. Yahyaev, U.V. Yusifova, Semiconductors, **44** (7), 904 (2010). DOI: 10.1134/S1063782610070134.
[6] D.A. Drabold, U. Stephan, J. Dong, S.M. Nakhmanson, J. Mol. Graphics Mod., **17** (5-6), 285 (1999). DOI: 10.1016/S1093-3263(99)00036-4
[7] B.A. Golodenko, A.B. Golodenko, Vestn. Voronezh. Gos. Univ. Inzh. Tekhnol., No. 2, 65 (2014) (in Russian). https://cyberleninka.ru/article/n/modelirovanie-elektronnoy-struktury-i-raschyot-osnovnyh-elektro-fizicheskih-parametrov-amorfnogo-kremniya
[8] V.B. Kvaskov, *Poluprovodnikovye pribory s bipolyarnoi provodimost'yu* (Energoatomizdat, M., 1988) (in Russian).
[9] T.L. Kulova, L.A. Mazaletskii, A.A. Mironenko, A.S. Rudyi, A.M. Skundin, Yu.S. Tortseva, I.S. Fedorov, Russ. Microelectronics, **50** (1), 45 (2021). DOI: 10.1134/S1063739720060074.
[10] P. Thomas, J.C. Flachet, J. Phys. Colloq., **42** (C4), C4-151 (1981). DOI: 10.1051/jphyscol:1981430
[11] H. Steinfink, B. Post, I. Fankuchen, Acta Cryst., **8** (7), 420 (1955). DOI: 10.1107/s0365110x55001333